

Supporting Information

NiMn Compound Nanosheets for Electrocatalytic Water Oxidation:

Effects of Atomic Structures and Oxidation States

Zhuwen Chen,^{a,b} Zheng Wang,^b Rongming Cai,^b Yangshan Xie,^b Jun Yu,^b Xia Long,^{b} Bo Yang,^{a*} Shihe Yang^{b,c*}*

1. College of Chemistry and Environmental Engineering, Shenzhen University, Shenzhen 518060, PR China. E-mail: boyang@szu.edu.cn
2. Guangdong Provincial Key Lab of Nano-Micro Material Research, School of Chemical Biology and Biotechnology, Peking University Shenzhen Graduate School, Shenzhen 518055, China. E-mail: xialong@pku.edu.cn, chsyang@pku.edu.cn
3. Department of Chemistry, The Hong Kong University of Science and Technology, Clear Water Bay, Kowloon, Hong Kong, China.

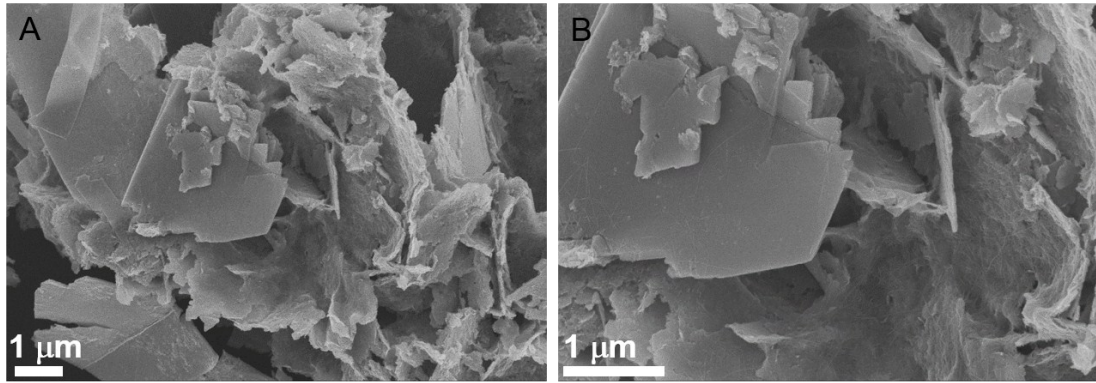


Figure S1. SEM images of Ni-birnessite showing the large nanosheet microstructure.

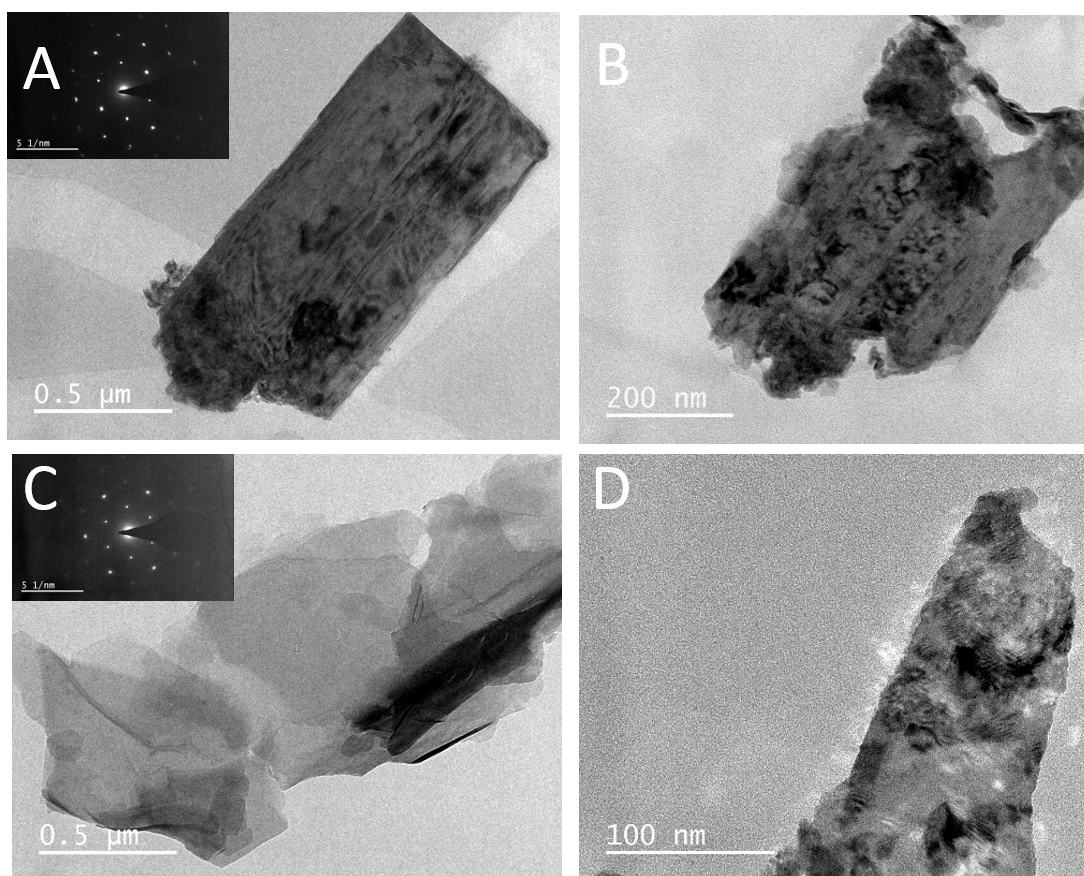


Figure S2. TEM images of (A) Ni-Birnessite, (B) NiMnO_x-B, (C) NiMn LDH and (D) NiMnO_x-L, insets are the SAED images of the corresponding samples.

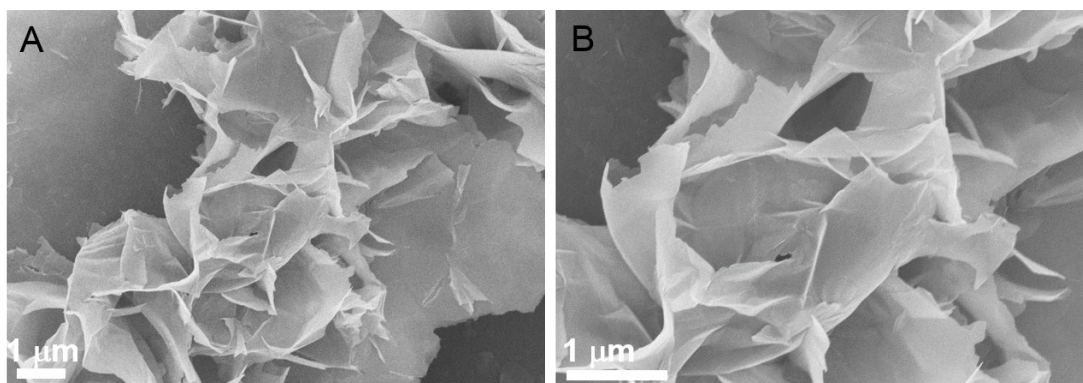


Figure S3. SEM images of NiMn LDH showing the thin nanosheet microstructure.

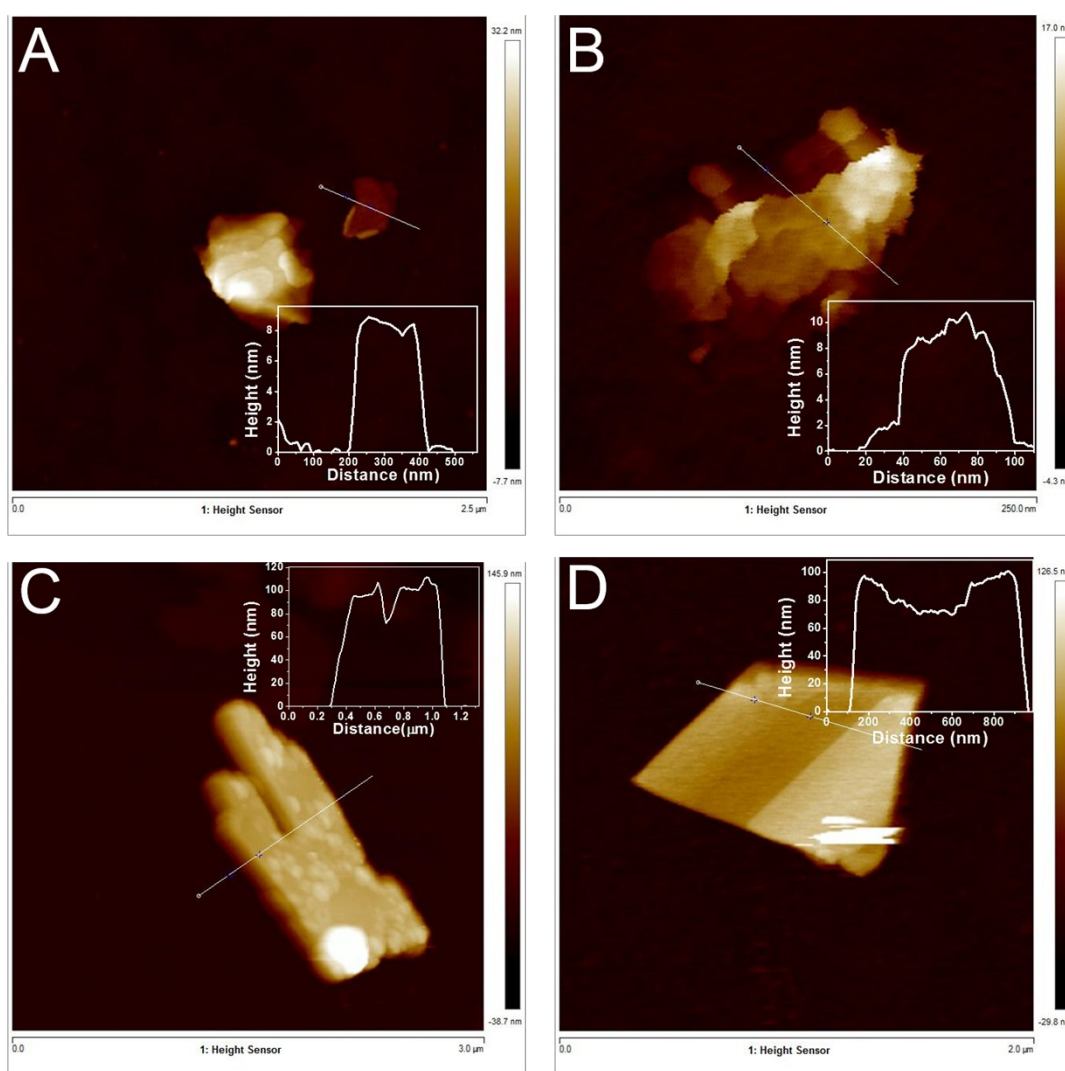


Figure S4. AFM images and the corresponding height profiles of the four NiMn compounds. A) NiMn LDH, B) NiMnO_x-L, C) Ni-birnessite, D) NiMnO_x-B. The thicknesses of NiMn LDH and NiMnO_x-L were less than 10 nm, and those of Ni-birnessite and NiMnO_x-B were ~100 nm.

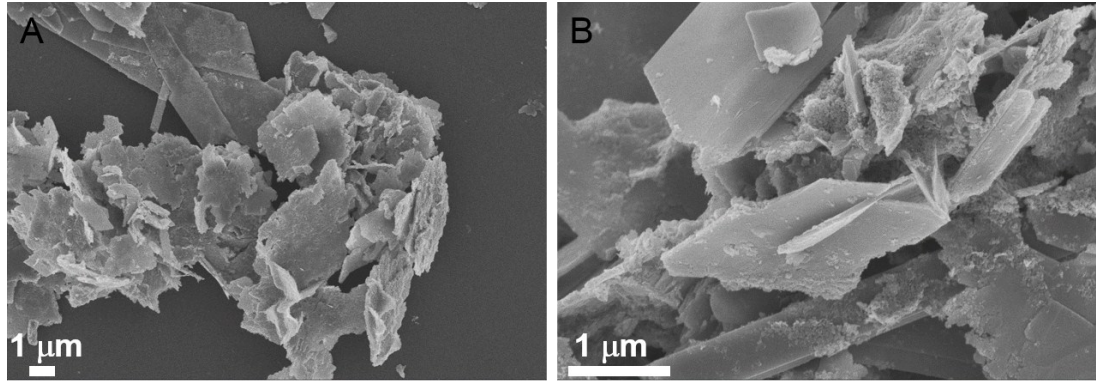


Figure S5. SEM images of NiMnO_x-B showing the retained nanosheet microstructure.

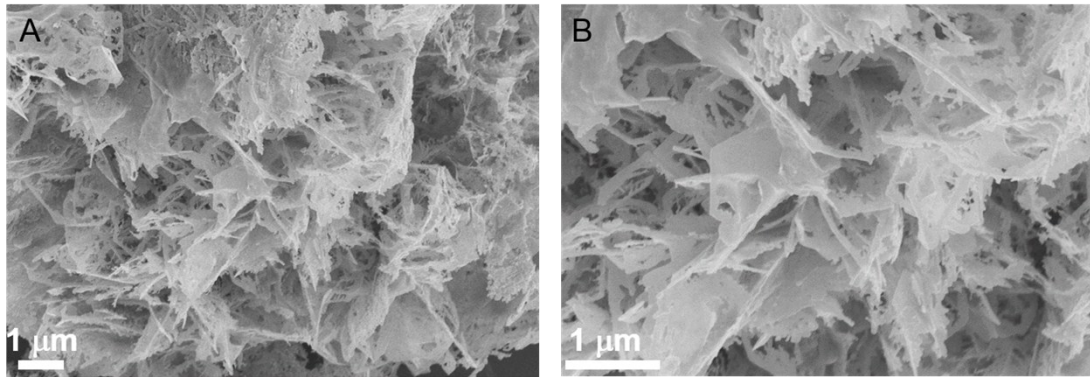


Figure S6. SEM images of NiMnO_x-L showing the porous nanosheet microstructure.

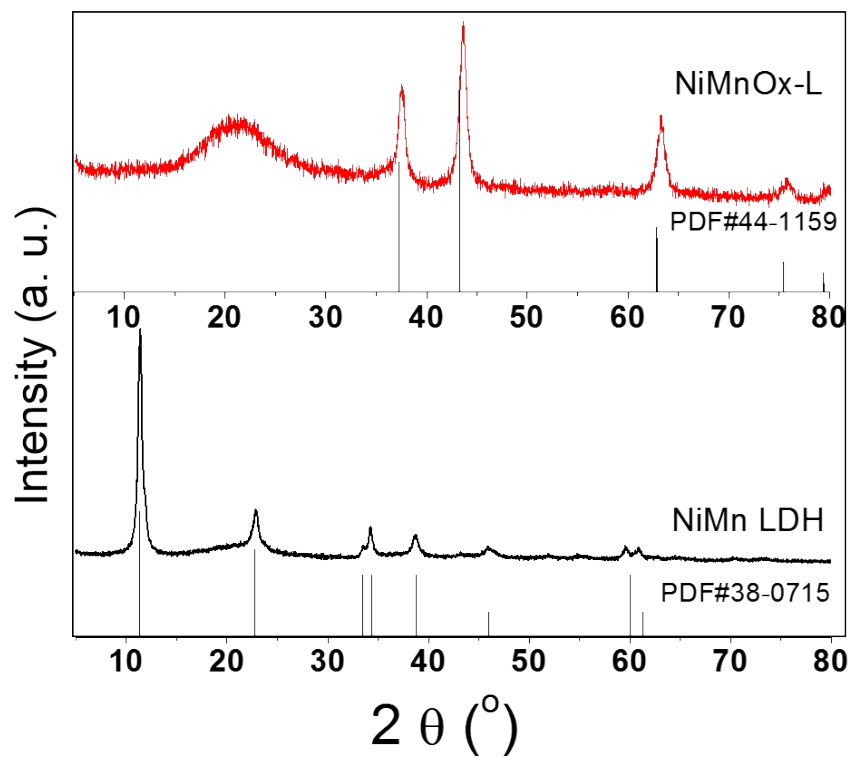


Figure S7. XRD spectra of NiMn LDH before (black curve) and after (red curve) the annealing treatment.

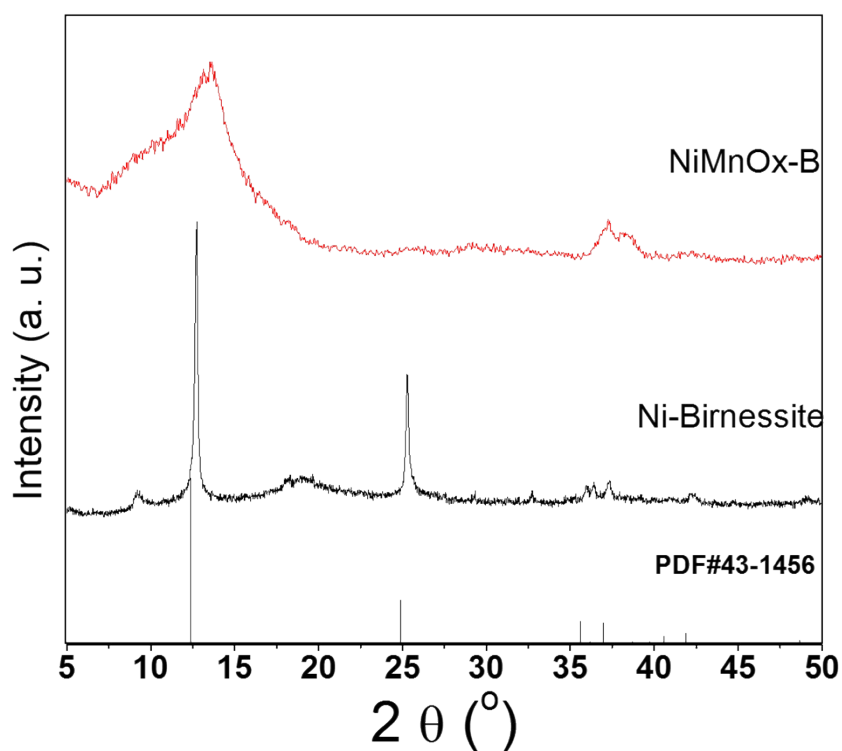


Figure S8. XRD spectra of Ni-Birnessite before (black curve) and after (red curve) the annealing treatment.

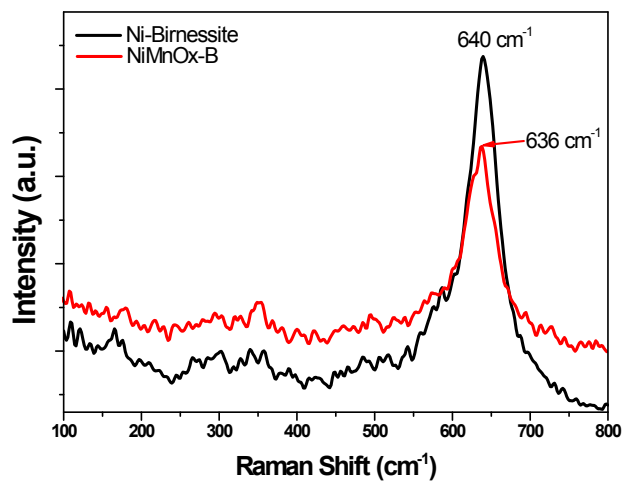


Figure S9. Raman spectra of NiMnO_x-B and its precursor of Ni-birnessite.

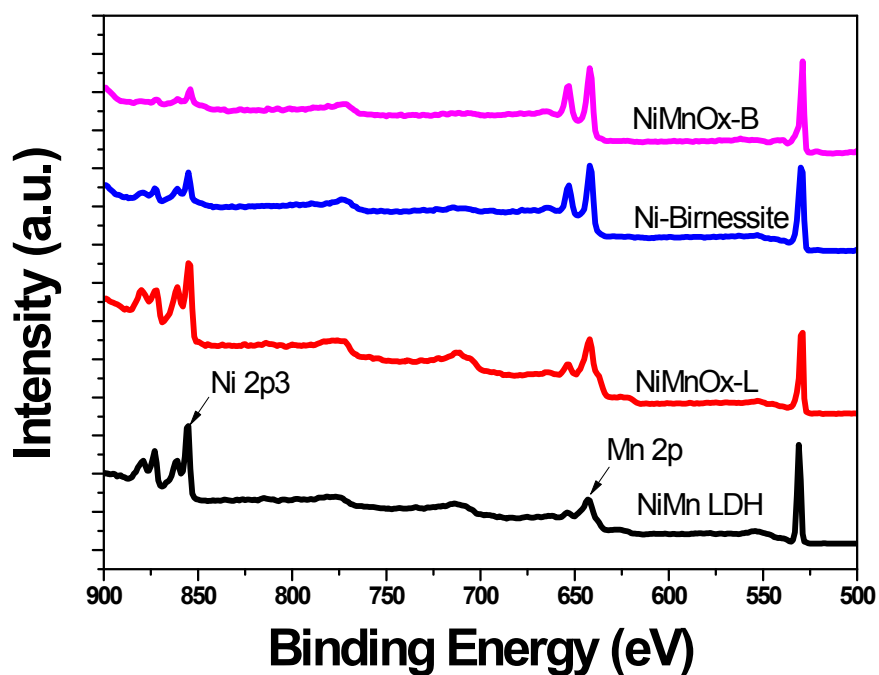


Figure S10. The full XPS spectra of the catalysts. The atomic ratio of Ni/Mn for Ni-birnessite, NiMn LDH, NiMnO_x-B and NiMnO_x-L is 0.44, 1.42, 0.24 and 1.32, respectively.

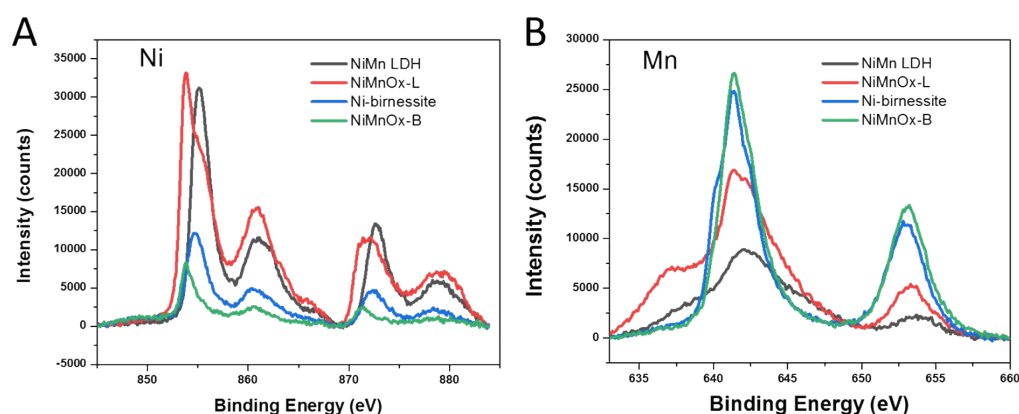


Figure S11. High resolution XPS spectra of the catalysts in (A) Ni, and (B) Mn 2p regions.

Table S1. Summary of the structure and performance of the as-prepared four samples.

	NiMnO _x -B	NiMnO _x -L	NiMn LDH	Ni-birnessite
Atomic structure	Layerd	Cubic	Layerd	Layerd
Morphology	Microsheets	Porous nanosheets	Nanosheets	Microsheets
Conductivity	2	3	1	4
ECSA	NiMnO _x -B > NiMn LDH > NiMnO _x -L > Ni-birnessite			
Ni/Mn	0.24	1.32	1.42	0.44
Ni (III)/Ni (II)	1.03	3.73	1.53	1.30
Mn (III)/Total	0.87	0.15	0.15	--
h (10 mA/cm ²)	362	383	386	412
Tafel slope	69	71	83	98

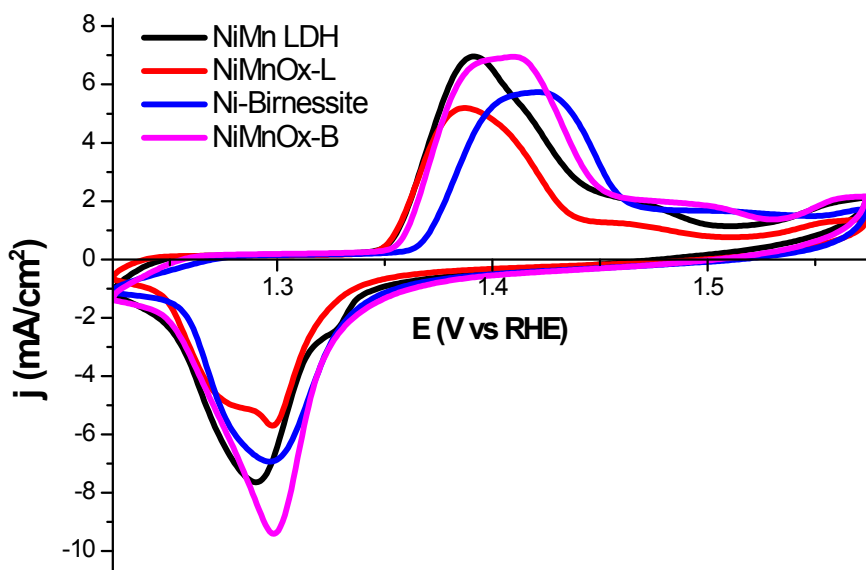


Figure S12. CV scanning curves of the as-made samples after 50 cycles.

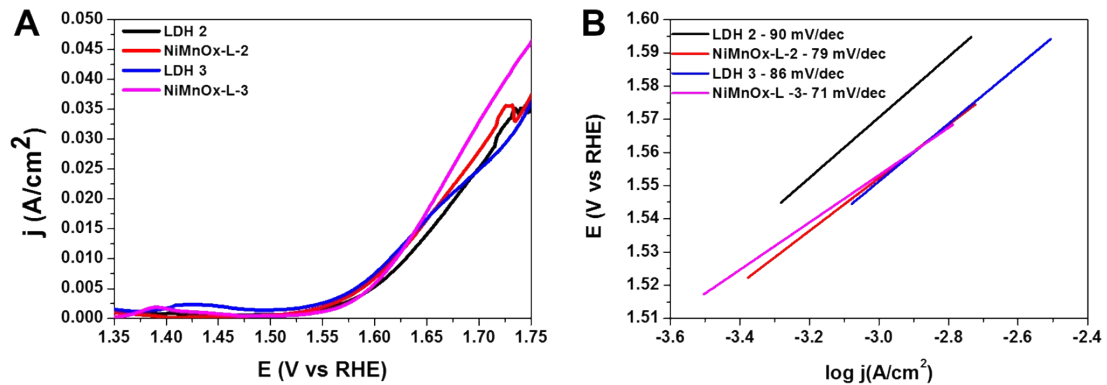


Figure S13. (A) LSV polarization curves, (B) Tafel plots of LDH samples synthesized with different Ni/Mn ratio precursor. By comparing to the LDH sample with a precursor Ni/Mn ratio of 1, the precursor Ni/Mn ratio of LDH 2 and LDH 3 was 0.8 and 1.6 respectively.

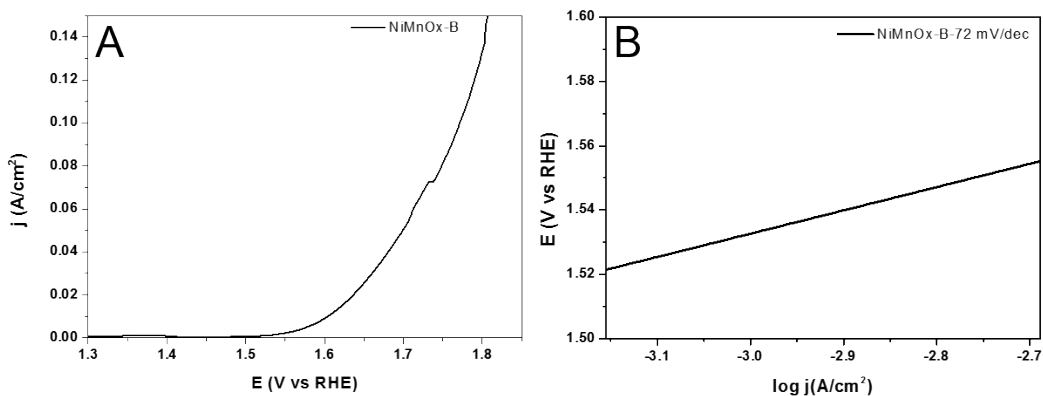


Figure S14. Electrochemical performance of NiMnO_x-B tested by using the graphitic rod as the counter electrode. (A) LSV curve, (B) Tafel plots.

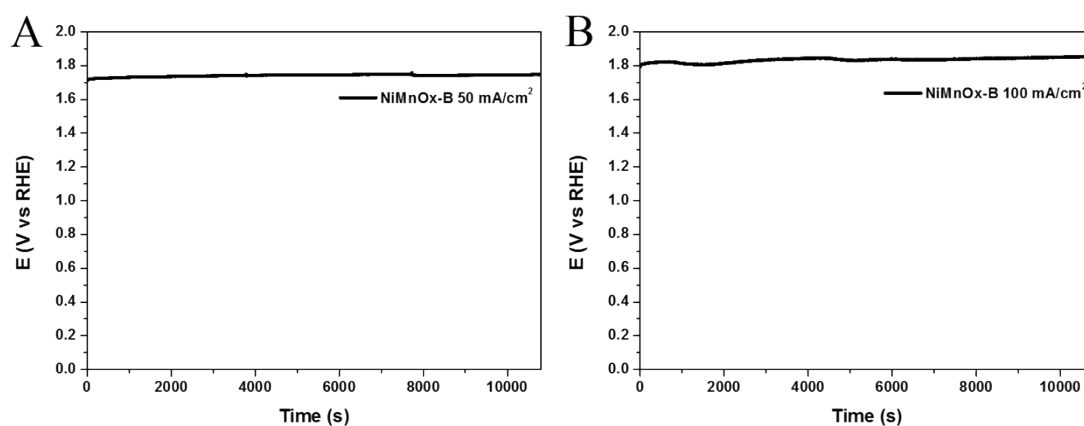


Figure S15. The stability testing result of NiMnO_x-B at the constant current density of 50 (left panel) and 100 mA/cm² (right panel) for more than 10000 s in even harsh conditions of 6 M KOH electrolyte and 60 °C temperature.

Table S2. ICP test of the 1M KOH solution after the electrochemical tests.

Samples	Concentration of metal (mg/L)		
	Pt	Ni	Mn
NiMnO _x -B	N.D.	N.D.	N.D.
NiMnO _x -L	N.D.	N.D.	N.D.

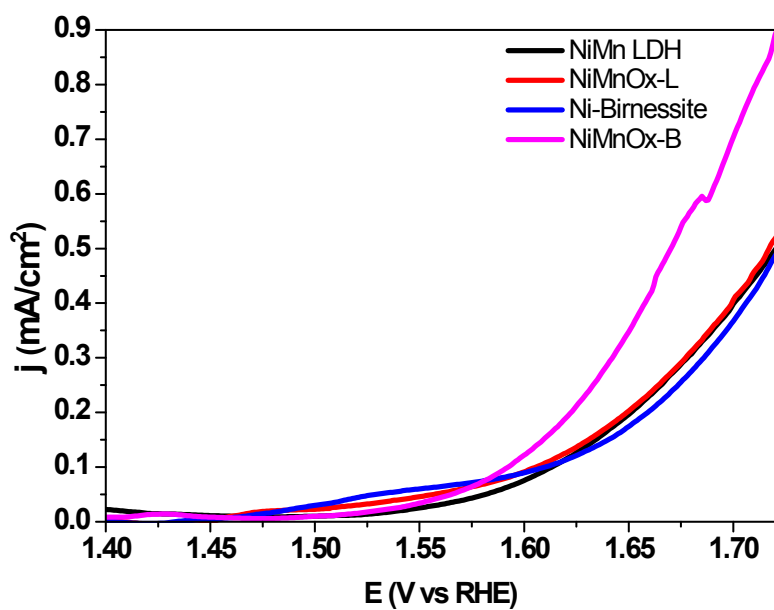


Figure S16. Calculated LSV using ECSA as values, and the ECSA can be calculated according to the formula $ECSA = C_{DL}/C_S$, where a specific capacitance of $C_S = 0.040 \text{ mF cm}^{-2}$ was used in this work.